Geological CO2 Capture and Storage with Flue Gas Hydrate Formation in Frozen and Unfrozen Sediments

Geological CO_2 Capture and Storage with Flue Gas Hydrate Formation in Frozen and Unfrozen Sediments: Method Development, Real Time-Scale Kinetic Characteristics, Efficiency, and Clathrate Structural Transition

Aliakbar Hassanpouryouzband[1], Jinhai Yang[1], Bahman Tohidi[1], Evgeny Chuvilin[2], Vladimir Istomin[2], and Boris Bukhanov[2]*

[1] Hydrates, Flow Assurance & Phase Equilibria Research Group, Institute of Petroleum Engineering, School of Energy, Geoscience, Infrastructure and Society, Heriot-Watt University, Riccarton, Edinburgh, EH14 4AS, UK.

[2] Skolkovo Institute of Science and Technology (Skoltech), 3 Nobel Street, Skolkovo Innovation Center, Moscow 143026, Russia

Abstract

The climate system is changing globally, and there is substantial evidence that subsea permafrost and gas hydrate reservoirs are melting in high-latitude regions of the Earth, resulting in large volumes of CO_2 (from organic carbon deposits) and CH_4 (from gas hydrate reserves) venting into the atmosphere. Here, we propose the formation of flue gas hydrates in permafrost regions and marine sediments for both the geological storage of CO_2 and the secondary sealing of CH_4/CO_2 release in one simple process, which could greatly reduce the cost of CO_2 capture and storage (CCS). The kinetics of flue gas hydrate formation inside frozen and unfrozen sediments were investigated under realistic conditions using a highly accurate method and a well-characterized system. The results are detailed over a wide range of temperatures and different pressures at in situ time scales. It has been found that more than 92 mol% of the CO_2 present in the injected flue gas could be captured under certain conditions. The effect of different relevant parameters on the kinetics of hydrate formation has been discussed, and compelling evidence for crystal-structure changes at high pressures has been observed. It has also been found that temperature rise leads to the release of N_2 first, with the retention of CO_2 in hydrates, which provides a secondary safety factor for stored CO_2 in the event of a sudden temperature increase.

*Corresponding author: petjy@hw.ac.uk

Introduction

Increasing atmospheric CO_2 concentrations, owing to the continuous use of fossil fuels as the main energy source for humans, pose a hazard to human life[1], possibly have a major role in global warming[2], may change environmental life cycles[3,4], and have long-term importance for the foreseeable future[5]. The increase in temperature in high-latitude regions of the Earth in particular appears to be occurring twice as fast as the global average[6], notably where vast volumes of CH_4 in the form of clathrates exist under permafrost[7] and where a significant amount of organic carbon is accumulated in perennially frozen soil over millennia[8]—a situation that will exacerbate climate change by extensive methane venting to the atmosphere[9] (which mainly comes from decomposition of gas clathrates) and by conversion of the stored carbon to CH_4 and CO_2 through decomposition by soil microbes[10]. Accordingly, urgent[11] action is required to scale-up CO_2 capture and storage to limit CO_2 emissions and return to a "safe"[6] level (1987) of 350 ppm CO_2 in the atmosphere. Although the efficiency of different techniques for CCS have been improved considerably in recent years[12], large-scale, economical solutions are still lacking[5].

In the past decade, a number of studies[13] have been undertaken to develop realistic CCS methods, one of which is using gas hydrate-related technologies. Gas hydrates, or clathrate hydrates, are an ice-like group of crystalline inclusion compounds characterized by a host lattice of hydrogen-bonded water molecules that enclose suitably sized guest gas molecules without chemical bonding, usually at low temperatures and elevated pressures[14–16]. Capturing and storing CO_2 in the form of gas hydrates has been previously suggested as a possible approach to reduce CO_2 emissions, which can be categorized into two main approaches: First, methane hydrate reservoirs that exist under permafrost and in continental and margin sediments[7] can be used to store CO_2[17] by replacement of injected CO_2 molecules with CH_4 molecules[18], controlling the emissions of CO_2 while simultaneously allowing for a more economical and more efficient[19] deployment of methane hydrate sources with respect to the exothermic[20] nature of CO_2 replacement in the hydrate lattice (This is due to the greater relative thermodynamic stability of CO_2 hydrate than both methane hydrate structure-I (sI) and structure-II (sII)). Furthermore, the optimization and development of this method have been extensively studied in the past two decades[21–23], and several successful field-scale applications, such as those located at the Alaska North Slope[24], have been reported. More recently, we have suggested direct injection of power plant flue gas (mainly N_2 and CO_2) into CH_4 hydrate reservoirs as a promising approach to reduce the cost by eliminating CO_2 capture from the atmosphere[25,26]. Second, efforts have been made to form gas hydrate from power plant flue gas[27], with the expectation that more CO_2 than N_2 will enter the hydrate phase[28–30], providing the possibility to separate and capture CO_2 after hydrate formation[31].

Here, we introduce a new approach to scale-up and reduce the cost of the CCS operation. The idea is that power plant flue gas, mainly consisting of N_2 and CO_2, can be directly injected into either simulated or natural (temporary and permanent storage, respectively) water/ice-saturated sediments at high pressures to store CO_2 in a solidified form, providing a realistic and efficient CCS method. Despite the promising prospects of hydrate-based CCS, a natural time-scale evaluation of flue gas hydrate formation kinetics inside mesoporous media does

not yet exist. This work details the results of an experimental investigation into the kinetics of flue gas hydrate formation in well-characterized water/ice-saturated sediments from 261.1 K to 283.1 K, covering the temperature range of subglacial, permafrost, subpermafrost, and subsea sediments[32]. Using the newly measured formation kinetics data, we discuss the characteristics of flue gas hydrate formation kinetics with a particular focus on the effect of relevant parameters on CO_2 capture rate, capture efficiency and clathrate stoichiometry.

This study documents a method that could slow or even stop the rise of the CO_2 content in the atmosphere. While direct formation of CO_2-rich hydrates from power plant flue gas will reduce CO_2 emissions, the hydrate cap formed in sediments could also provide a safety[33] mechanism by blocking the pathway of those greenhouse gases released in response of permafrost to global warming. Additionally, we address the challenges regarding the effect of global warming on the stored CO_2-rich hydrates by investigating the kinetics of hydrate dissociation during temperature increase, ultimately showing that the CO_2 level in the atmosphere could be sustainably reduced or at least kept at the same level using the proposed method.

Methods

Materials

A well-characterized silica sand from Fife (Scotland) was used as the mesoporous media, and a detailed analysis can be found in the Supporting Information. Deionized water was produced using an ELGA DV 25 Integral Water Purification System. For simulating flue gas, a gas mixture composed of 85.4 mol% nitrogen and 14.6 mol% CO_2 (both with certified purities of 99.9995 vol%) purchased from BOC Limited was used.

Experimental apparatus

Experiments were carried out using a stainless steel cylindrical cell setup. The setup is composed of a high-pressure cell (with a maximum inner volume of 802 cm3 and a maximum working pressure of 40 MPa), movable piston, data measurement and monitoring system, and pressure/temperature maintaining system, as shown in Fig. 1. The top cap of the cell is fixed, while the bottom cap has a movable piston, moving by injection or withdrawal of hydraulic fluid using a hand pump for initial overburden pressure and a Quizix pump for maintaining constant pressure. The piston movement enables an increase or reduction in the pore pressure within the cell without injecting or removing fluid from the cell, thus maintaining a closed system. A linear variable differential transformer (LVDT) is mounted to the tail rod of the piston to measure the piston displacement, enabling measurement of the exact volume of the cell in real time. The cell is located in a cooling jacket, and its temperature is maintained by circulating water/monoethylene glycol ((60/40, vol/vol) from the temp bath (Julabo MA-4) through the shell side of the module. The temperature is measured using a platinum resistance thermometer (PRT), located inside the top cap, with a precision of +/- 0.1 K. The cell pressure and overburden pressure are measured by means of Quartzdyne pressure transducers (model QS30K-B, Quartzdyne Inc., U.S.A., pressure range 0-207 MPa) with an accuracy of +/- 0.0005 MPa. Pore pressure, temperature, pump pressure, overburden pressure, and piston displacement are recorded on a computer via a data acquisition system

(LabVIEW software from National Instruments). Test fluids and samples for analysis are injected and collected through valves on the bottom cap, top cap, and side valves. The molar composition of the gas samples was analyzed using a gas chromatograph (GC) (Varian 3600, Agilent Technologies) (with calibration errors of ±0.5% for CO_2 and ±1.2% for N_2).

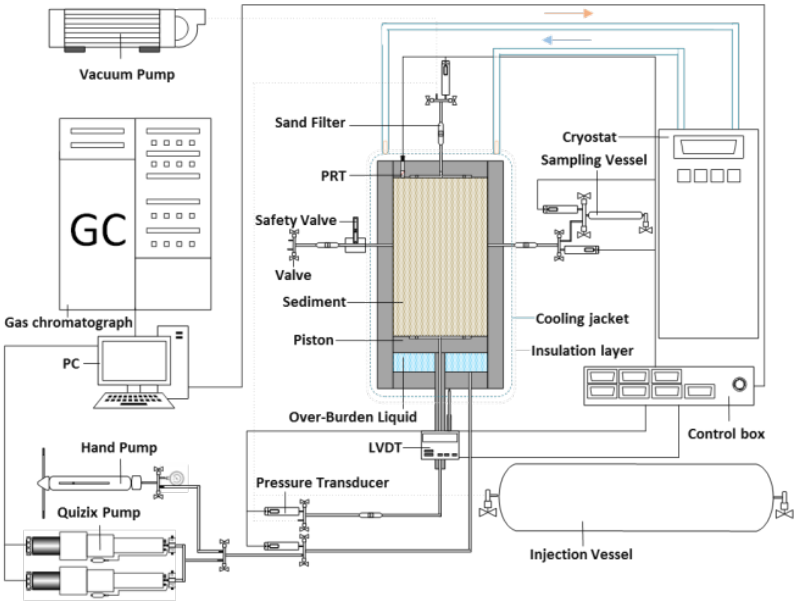

Fig. 1 Schematic of the high pressure autoclave setup

Procedure

The following general procedure was used for all experiments. The cell was filled with partially water-saturated sand (1076.6 g sand/155.6 g water or 12.63 mass% water) and vacuumed after adjusting the piston level to control the volume of simulated sediment (approximately 148.94 mm height and 75.00 mm diameter or porosity of 37.9%). The fluid behind the piston was then maintained at a constant pressure (3.45 MPa) using the Quizix pump and the temperature bath was set at the target temperatures (see Table 1) for several days to ensure stabilization of the system. Then, the piston fluid inlet valve was closed, and flue gas was injected at the desired pressures. Gas samples for GC were collected at determined intervals according to the pressure decrease rate of the system. The sampling process was continued until hydrate formation finished, as evidenced by both the final stable CO_2 concentration in the gas phase and the pressure reading of the pressure transducer[28], except for Exp1, in which the test was stopped after 72 days because of the very slow formation rate. Finally, the bath temperature was set at 294.15 K, and the composition of the gas phase was analyzed during gas hydrate dissociation. The initial conditions for each experiment are shown in Table 1.

Table 1 Experimental temperature, initial pressure conditions, and quantity of injected gas

Exp. No	1	2	3	4	5	6	7	8	9
Temperature (K)	261.2	264.8	268.6	273.4	278.2	283.2	273.4	278.2	283.2
Start Pressure (MPa)	20.82	20.79	20.81	20.79	20.75	20.80	27.95	27.91	33.21
Injected Gas (mol)	1.0198	0.9974	0.9761	1.0009	0.9476	0.9111	1.2574	1.1974	1.3137

Methodology

Pure CO_2 forms simple (single guest) cubic sI clathrate hydrates with a formula of $2M_S \bullet 6M_{LI} \bullet 46H_2O$ (where M_S is a small 5^{12} (pentagonal dodecahedron) cavity and M_{LI} is a large $5^{12}6^2$ (tetrakaidecahedron) cavity) with compositions between $5\frac{3}{4}$ and $7\frac{2}{3}$ waters/guest, which are stable at considerably lower pressures when compared with simple N_2 hydrates. CO_2 occupies all the large M_{LI} cages (size ratio of 0.83) and some of the M_S cages (size ratio of 1). Additionally, N_2 can stabilize cubic s-II hydrates with a unit cell formula of $16\ M_S \bullet 8M_{LII} \bullet 136H_2O$ (where M_{LII} is a large $5^{12}6^4$ (hexakaidecahedron) cavity), occupying a fractionally higher number of M_S cavities (single guest)[34]. In addition, owing to the small molecular size, two N_2 molecules can fit into a large M_{LII} cavity[35,36]. While several powder X-ray diffraction, NMR spectroscopy, and Raman spectroscopy studies[37–39] (mainly on 10% and 20% CO_2 in N_2+CO_2 mixtures) at limited pressure and temperature ranges suggest that these mixtures only form s-I hydrate (except for 1% CO_2-99% N_2 mixture where the s-II hydrate is more stable), structures of CO_2+N_2 mixed hydrates have yet to be investigated to reveal the underlying physics. At the same time, the presence of mesoporous media can change the characteristics of hydrate equilibria[40]. Accordingly, this is another key parameter to be analyzed in order to understand the properties of CO_2+N_2 hydrate formation inside sediments.

Fig. 2 provides the predicted results of sI and sII HSZs of gas-water systems for different combinations of CO_2 and N_2 together with the pressure/temperature conditions of the experiments. To understand the effect of temperature under real conditions[32], Exp 1-6 were started at the same pressure, which was selected to represent ocean floor pressure according to the average depth of the oceans[41,42]. Exp 7-9 were performed to investigate the pressure effect. It should be noted that as all planned results were obtained using these 9 experiments, we performed only one experiment at very low temperature due to the length of time required to perform experiments at lower temperatures and higher pressures. The pressures for Exp 1-4 and 7 were well inside the N_2 HSZ, whereas the pressures for Exp 5 and 9 were between the flue gas and N_2 HSZs, the pressure for Exp 8 was just on the N_2 HSZ, and the pressure for Exp 6 was outside of the flue gas hydrate formation region. Accordingly, in Exp 1-5 and Exp 7-9, there is the possibility of CO_2 or CO_2-N_2 mixed hydrate formation, and in Exp 1-4 and 7, there is also possibility of N_2 hydrate formation. The sole purpose of Exp 6 was to observe CO_2 dissolution kinetics in the system. For some combinations of flue gas (sometimes up to ~8% CO_2 at lower temperatures), the pressures of sII HSZs are lower than those of sI, indicating the greater stability of sII hydrates from a thermodynamic perspective. Accordingly, Exp-5 and 9 were selected to be out of this region, whereas other experiments (except Exp 6) cross this region or finish (Exp 1 and 7) in this region. Several experimental obserevations[20], all of which were performed outside of this region, suggest that CO_2 will go into large cages and N_2 will occupy small cages (for sI hydrates) in CO_2-N_2 mixed hydrates.

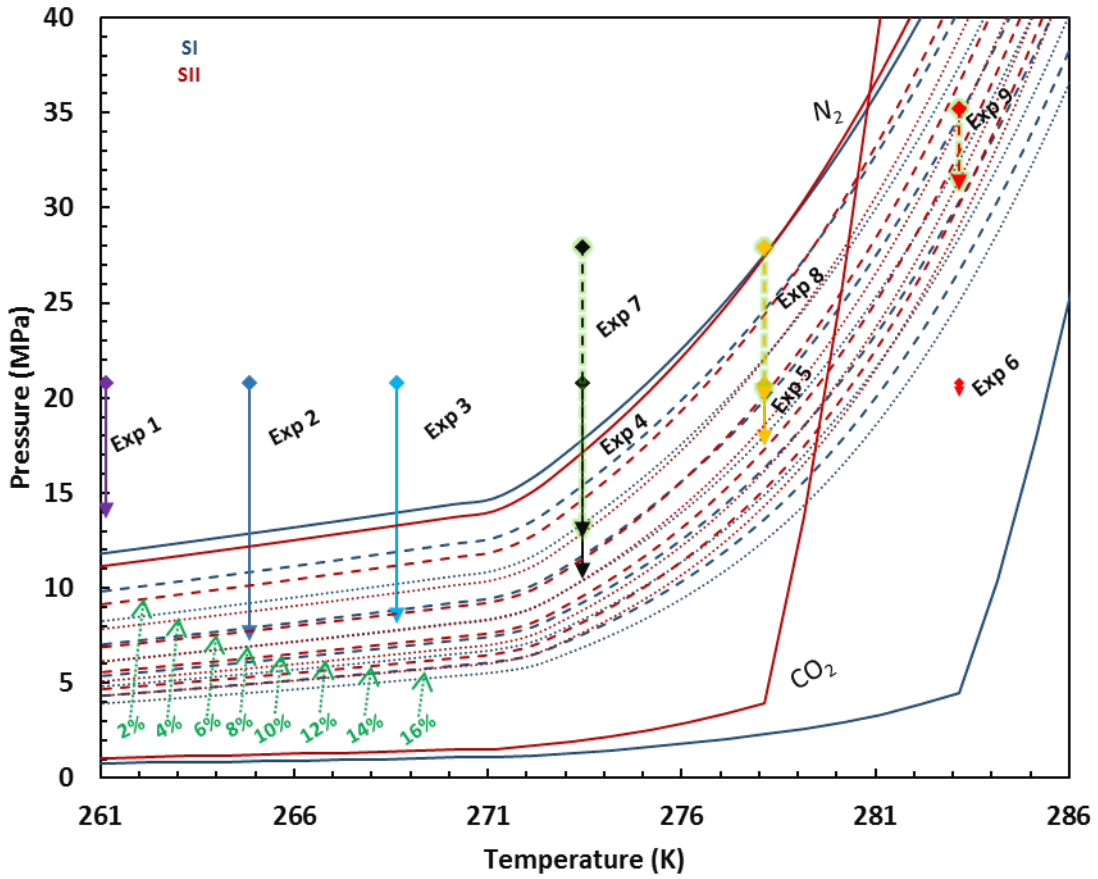

Fig. 2 The predicted hydrate stability zones of CO_2, N_2, and their mixtures and the experimental conditions. The HSZs are predicted for both sI and sII. The paired phase boundaries of sI and sII of a CO_2-N_2 mixture are drawn in the same pattern of lines, blue (sI) and red (sII). An in-house software was used for prediction of the HSZs[43–45]. Thermodynamic behavior of the fluid system at different pressures, temperatures and compositions were modelled using CPA equation of state for the non-solid phase, with the Peng-Robinson equation of state as the non-association part, and a modified van der Waals and Platteeuw method for the solid phase.

Results and Discussion

Formation kinetics

The pressure profile of the system after gas injection is illustrated over all of the experimental periods in Fig. 3. A rapid pressure drop was observed just after gas injection, mainly as a result of gas solubility and gas contraction. This mechanism is clearer in the Exp 6 results, where the system pressure was outside the flue gas HSZ. However, in the other experiments, hydrate nucleation/growth was an additional reason for this initial reduction. As the gas was consumed by hydrate formation, the gas pressure showed a strongly negative decreasing slope. Here, the rate of gas pressure change decreased with time, corresponding to a reduction in the gas consumption rate. This is because the consumption of the gas molecules moves the system pressure closer to stable conditions, reducing the main driving force of hydrate formation. Furthermore, early hydrate crystal formations accumulate on the surface,

reduce the surface contact of components and limit the mass/heat transport in the system. In addition, the free water content in the system reduces with hydrate formation, which could limit the hydrate formation rate by slowing down the adsorption of the CO_2/N_2 molecules at the crystal interface[46]. With regard to the pressure decrease during hydrate formation in Exp 3-5, it is slightly faster at lower temperatures, as the distance from stable conditions is relatively higher in terms of pressure difference (higher sub-cooling). However, the opposite trend was observed in Exp 1-2. This could be explained by the presence of less unfrozen (quasiliquid) water at lower temperatures. The quasiliquid water content acted as a limiting factor for hydrate formation and gas diffusion in the system, and consequently, a reduction in the hydrate formation rate at lower temperatures can occur. In addition, the gas diffusion rate is reduced at lower temperatures, which, in turn, increases the time required for gas molecules to contact the quasiliquid water. Furthermore, hydrates can directly form from ice crystals, which is slower at lower temperatures. Comparing the graph for Exp 3 with those for Exp 1 and 2 in Fig. 3 suggests that there was enough quasiliquid water and sufficient surface contact between components in Exp 3, weakening the limiting effects on hydrate formation at this temperature. As seen, except for Exp 1, the pressure graphs for all experiments reached a plateau after the initial decrease, which was faster at higher temperatures. This can be attributed to the fact that the differences between hydrate formation rates are not large enough to cover the difference between stable pressure values. In Exp 1, as the hydrate formation rate decreased considerably after a few months, the tests were stopped when the pressure versus time slope reached less than 0.0015 MPa/hr.

A comparison between the pressure decreases in Exp 4 and 5 with those of Exp 7 and 8 reveals that experiments at higher pressure take more time to stabilize. The first apparent reason for this observation is the pressure drop and consequently more hydrate formation at higher pressures. This can also increase the force required for diffusion through formed hydrate shells. As the same amount of water was present in all experiments, the second reason for this observation could be the previously discussed limiting role of free water, lowering the water to gas molar ratio at higher pressures. This is potentially the main reason for the very slow hydrate formation during the final stages of the higher pressure experiments. The faster hydrate formation in Exp 9 compared to Exp 7 and 8, considering its higher pressure and higher temperature, provides additional support for the above two explanations.

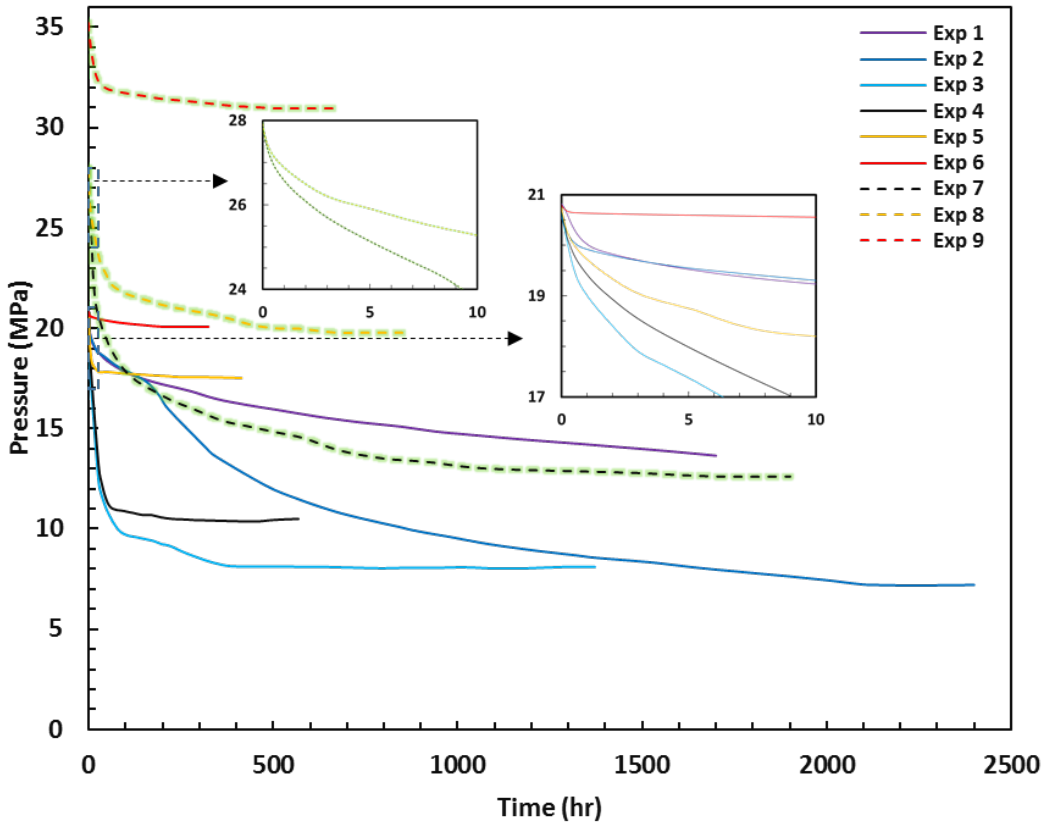

Fig. 3 Changes in system pressure after flue gas was injected during clathrate formation inside water saturated sediments with the early phase magnified.

CO_2 capture

Fig. 4 presents the CO_2 concentration changes in the gas phase throughout all experiments. An insertion of the initial stage is also shown in Fig. 4. It should be noted that all samples were analyzed at least three times to reduce the GC measurement uncertainty, which was calculated to be at most 0.1%. As shown in Fig. 4, there is always an initial decrease in CO_2 concentration in all cases due to the higher solubility of CO_2 relative to N_2 in the aqueous phase at temperatures higher than 273.15 K (Exp 4-9) and higher stability of CO_2 relative to N_2 in the ice phase at temperatures under 273.15 K (Exp 1-3). Furthermore, it is clear that the relative rate of diffused CO_2 to N_2 into the ice phase is similar in Exp 1-3, indicating an insignificant role of temperature on the diffusion of gas into the ice crystals, at least in the early stages. However, for experiments above the freezing point of water (Exp 4-9), the relative rate of CO_2 to N_2 solubility in water increases at lower temperatures, due to hydrate formation requiring an induction time because there is always a time lag for hydrate formation after flue gas injection. As shown in the magnified part of Fig. 4, clear downward peaks were observed for Exp 4, 5, 7, 8, and 9 just after flue gas injection was complete. Previously, we reported[28] this behavior for the same gas mixture under bulk conditions and attributed it to the effect of hydrate formation on water solubility and the presence of relatively more CO_2 to N_2 in the aqueous phase than in the hydrate phase. Regarding Exp 6,

following approximately 200 hrs of initial logarithmic reduction, it reaches equilibrium at approximately 10.5% CO_2 in the gas phase.

The curves shown in Fig. 4 provide other interesting information. The curves show that the CO_2 concentration in the gas phase reduced considerably faster in Exp 4 and 5 than in Exp 1-3. At the same injection pressures for higher temperatures, the CO_2 concentration reached a stable value faster. However, the final CO_2 concentration in the gas phase is smaller at lower temperatures, indicating a higher occupancy ratio of CO_2/N_2 in the hydrate phase. Slower changes in the CO_2 concentration were observed at higher pressures, which could be attributed to the same reason for the slower pressure change in these systems. In addition, the presence of more gas in the system leads to a reduced effect of hydrate formation on the changes in the composition of the gas phase. Although Exp 9 was conducted under higher pressure than Exp 6, there was a higher rate of CO_2 capture in Exp 9, indicating the efficiency of hydrate-based CO_2 capture compared with dissolution methods alone. Comparing Exp 4 with Exp 7 and Exp 5 with Exp 8, it should also be noted that the injection of gas at higher pressures caused a greater reduction in pressure, which in turn led to more hydrate formation and consequently a larger change in the CO_2 concentration. Accordingly, experiments at higher injection pressures in this method also have higher final equilibrium pressures. This is because binary N_2/CO_2 gases have higher HSZs at higher N_2 concentrations.

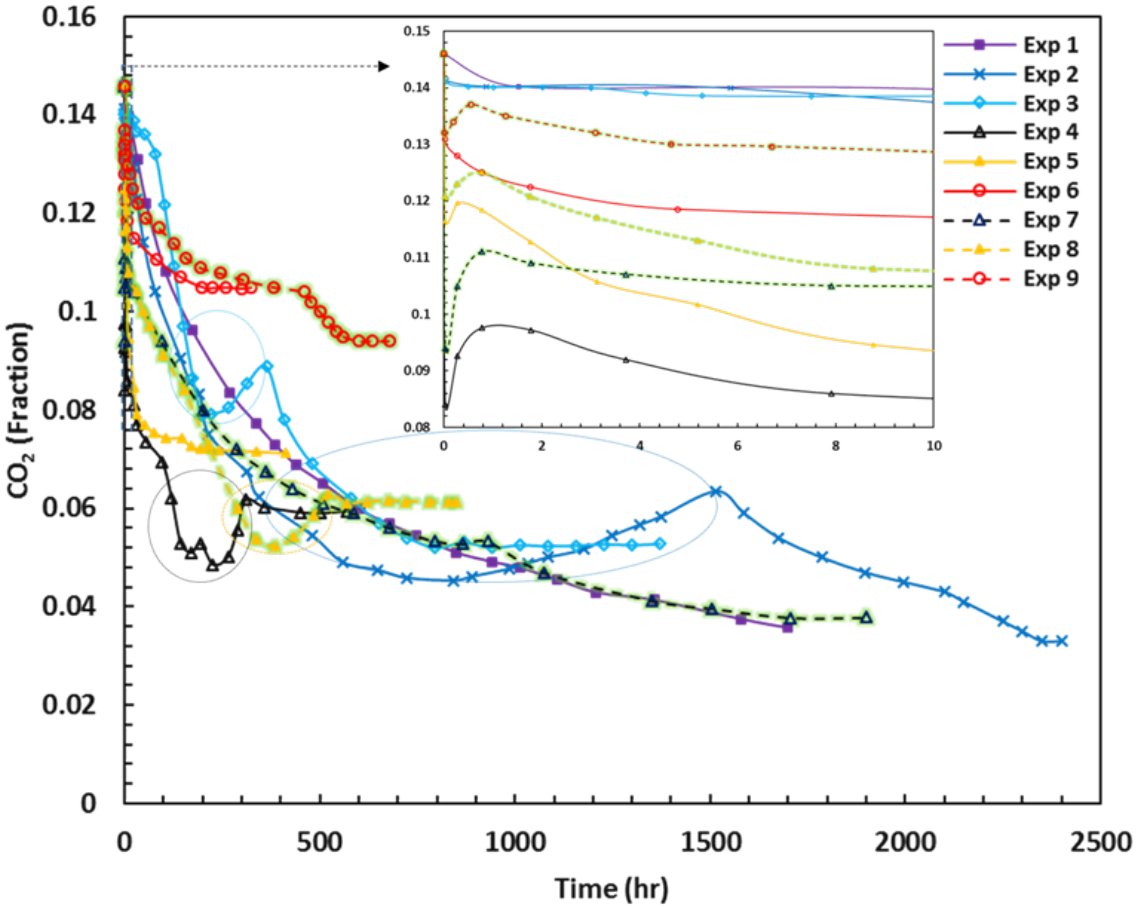

Fig. 4 Changes in CO_2 concentration in the gas phase during clathrate formation inside water saturated sediments after flue gas was injected. To reduce the GC measurement uncertainty for each point, all samples were analyzed at least three times.

Structural change

Next, we investigated the CO_2 concentration change during hydrate formation to further quantify the kinetics of flue gas hydrate formation. The important observation from comparison of the graphs in Fig. 4 is that there are concavities (circled parts) on CO_2 concentration in Exp 2-4 and 8. The possible explanation for these concavities is that these experiments were started inside the N_2 HSZ and finished outside of the N_2 HSZ, covering a wide range of HSZs in terms of concentration changes, which reduces the stability of hydrates formed at higher pressures. With this in mind, initially formed hydrates with relatively more CO_2 possibly dissociated, and new hydrates with less CO_2 formed. Curiously, the presence of more CO_2 at higher pressures indicates that there is an optimum pressure under which there is maximum CO_2 capture, which is consistent with our previous results[26]. Furthermore, a wider concavity in Exp 2 could show limited heat or mass transfer for dissociating hydrogen bonds at lower temperatures.

More interestingly, as shown in Fig. 4, HSZ zones of sII hydrates with CO_2 concentrations less than approximately 8% are more stable than those of sI, and the trend is opposite after

passing approximately 8% CO_2 in the gas phase. In addition, these concavities are observed only in Exp 2-4 and 8 that passed this region (Exp 1, 5, and 7 were above or inside this zone). On the basis of the two above explanations, for Exp 2-4 and 8 sII hydrate formation is the only plausible hypothesis that could be offered to explain the reason behind the concavities observed in Fig. 4. This does not conflict with other studies[37–39] on this subject that denied the presence of sII hydrate for more than 1% CO_2 concentration in the gas phase because the presented pressure-temperature conditions in our study for sII hydrate were not investigated in other studies. To confirm the structural changes, these experiments could be coupled with different spectroscopy techniques such as NMR to be able to measure the composition of the hydrate phase during formation.

Pressure effect on CO_2 capture

The rate of CO_2 capture is highly sensitive to variations in pressure at each temperature. Fig. 5 summarizes the changes in CO_2 concentration in the gas phase versus pressure under the conditions presented in the experimental section. Different parts of this figure were discussed in the previous sections. However, there are some interesting observations to be further addressed. The changes in the fraction of CO_2 in the gas phase is a measure of the relative stability of CO_2 to N_2 in the hydrate phase with respect to the pressure under which they form. The CO_2 concentration stays at approximately 14% in Exp 3 before reaching N_2 HSZ, whereas it begins reduction earlier in Exp 1 and 2. This could be explained by the presence of less quasiliquid water at the gas-water interface in Exp 1 and 2 and significantly higher stability of CO_2 than N_2 in the process of hydrate crystals accumulation at the gas/water interface, and the diffused gas contains a higher concentration of CO_2, in turn, leading to the formation of CO_2-rich hydrates. Because of the intensity of the lower temperature in Exp 1, the hydrate formation rate is very slow (Fig. 5), whereas the slope of CO_2 concentration versus pressure is high (Fig. 5). Furthermore, the CO_2 concentration significantly changes at the final pressure in Exp 2-5 and 7-9, which is most clear in Exp 3. Recently, we suggested[28] three different mechanisms for this behavior. In support of our above claims about the presence of sII CO_2-N_2 hydrates at higher pressures, the concavities of the curves in Fig. 5 are consistent with the stability regions of sII hydrates in Fig. 2.

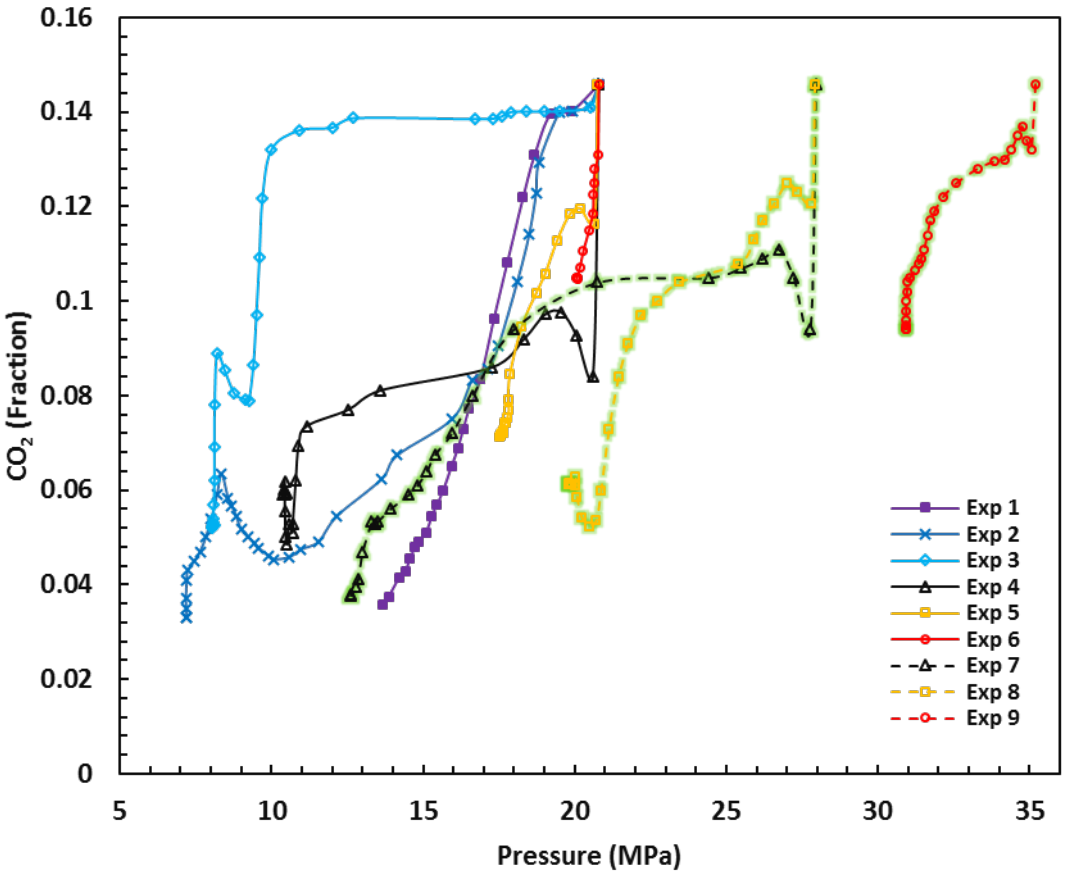

Fig. 5 CO2 concentration in the gas phase versus system pressure during clathrate formation inside water saturated sediments. The changes in the fraction of CO2 in the gas phase is a measure of the relative stability of CO2 to N2 in the hydrate phase with respect to the pressure under which they form

Quantitative analysis

Because the initial and final pressures and CO_2 concentrations in each test were different, there was a need to define a parameter to be able to comparatively quantify the amount of captured CO_2. Accordingly, the capture ratio, C-value, is defined as the percentage of captured CO_2 moles inside the hydrate and water phase divided by the moles of initially injected CO_2. The C-values for each experiment were calculated and plotted in Fig. 6 (quantities of the CO_2 concentration in the gas phase and hydrate/water phase are provided in the Supporting Information). As noted before, in Exp 1, the test was stopped before reaching the final pressure, so the C-value for this test does not reflect equilibrium conditions. It is clear from the graph that either an increase in the pressure or a reduction in the temperature caused an increase in the efficiency of the CO_2 capture, confirming the results shown in Fig. 4. Hence, lower temperatures and higher pressures are more favorable for CO_2 capture if the hydrate formation time is not important, which is applicable in this case. An apparent trend of C-values indicates that it is possible to store more than 92% percent of the injected CO_2 by controlling pressure and by choosing an appropriate area for storage. The separation of CO_2 from flue gas before injection does not seem to have any significant impact

in this method on increasing the capture ratio, while the separation of CO_2 from flue gas has a major[13] cost in typical CCS operations. Another interesting observation from Fig. 6 is that injection of flue gas into frozen sediments could even capture and store more CO_2 from the injected flue gas, which suggests that hydrate formation plays a dominant role over CO_2 solution in water.

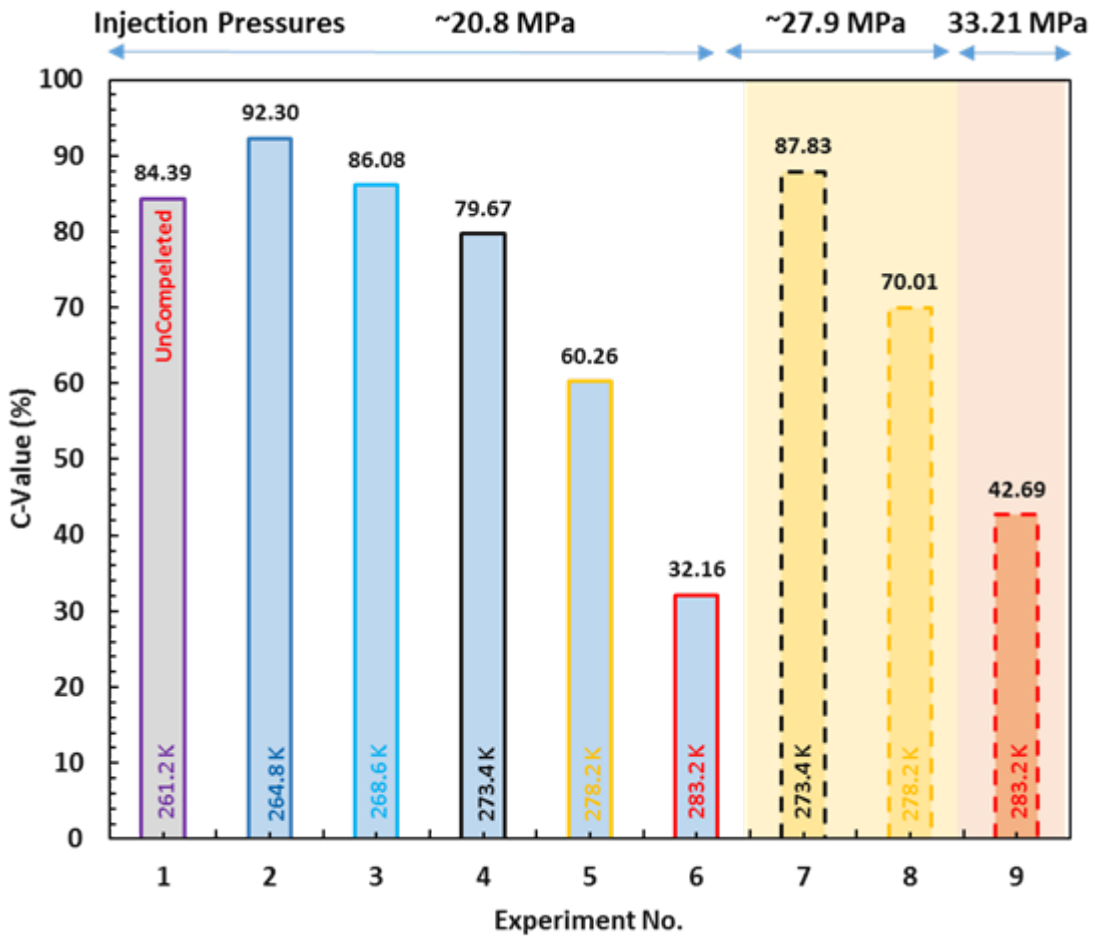

Fig. 6 C-value variations under different experimental conditions. An apparent trend of C-values indicates that it is possible to store more than 92% percent of the injected CO2 by controlling pressure and by choosing an appropriate area for storage.

Dissociation of CO_2-N_2 mixed hydrates

To further understand the effect of environmental temperature changes during natural cycles or the effect of any sudden climate changes such as the hypothesis of Late Quaternary climate change[47] on the stored hydrates, the composition of the gas phase during dissociation of the formed hydrates was examined at the end of the tests after setting the cryostat to room temperature (294.15 K). As the temperature increased, the gas started to expand and hydrate dissociation began, causing CO_2 concentrations to change in the gas phase, as shown in Fig.

7. Under frozen conditions (Exp 1-3), a constant CO_2 concentration was maintained and even slightly decreased at initial pressures after initiation of hydrate dissociation, which was followed by a fast release period. The decrease in the CO_2 concentration and relative stability of the CO_2 concentration range in terms of pressure change are both greater at lower temperatures. Especially for Exp 1, the CO_2 concentration in the region of relative pressure stability region is more than 60% of the total pressure rise by heating. The relative stability of CO_2 at early stages under frozen conditions suggests that more energy (in the form of heat) is required to overcome energy barriers and destabilize the CO_2 than N_2 inside clathrate cages. The rate of CO_2 concentration change for this experiment, however, is considerably higher during the second phase. This supports the conclusion that after the formation of N_2-rich gas hydrate at the water-gas interface, CO_2-rich gas hydrate formed inside the initially formed hydrate shells, which is in agreement with the above results of hydrate formation. Furthermore, the trends of CO_2 concentration change during hydrate dissociation generally follow the opposite pressure path from that in which they formed. During dissociation, the CO_2 concentration changes have a less steep slope at lower pressures and generally increase at higher pressures. This is one of the strongest advantages of this method because during small temperature changes, considerably more N_2 than CO_2 will be released, reducing the hazard from CO_2 release and increasing the safety associated with temperature changes. As an additional support for clathrate structural change in Exp 2-4 and 8, there are sharp changes in the slope of the curves (circled part) only for these experiments, which are missing for the other ones. Finally, sharp drops in the CO_2 concentration at the end of the dissociation experiment are clearly from the dissolution of CO_2 in the water phase.

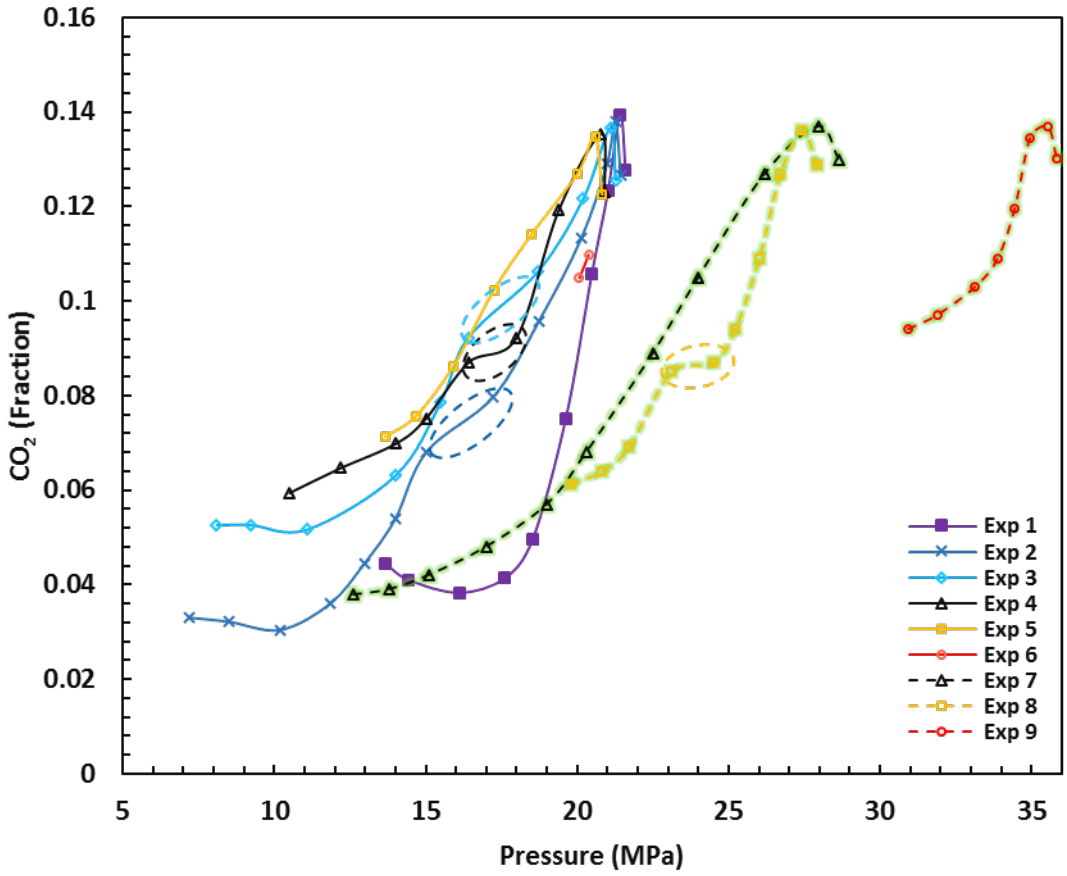

382

383 **Fig. 7** CO_2 concentration in the gas phase versus system pressure during hydrate dissociation after
384 bath temperature was set to 294.15 K.

385

386 In summary, we proposed an innovative approach for geological CCS by direct injection of flue
387 gas into water/ice-bearing sediments in the absence of initial methane gas hydrates in place,
388 integrating CO_2 capture and storage into one simple process, and consequently reducing the
389 cost of CCS significantly by comparison with conventional gas hydrate-based CCS methods.
390 Here, the presence of N_2 in the feed gas facilitates the movement of the gas and reduces the
391 corrosion of facilities in comparison with supercritical CO_2. The proposed method shows very
392 high efficiency, with greater than 92% stable CO_2 capture under certain conditions, meeting
393 the technical requirements of typical industrial-scale geological CO_2 storage operations
394 reported in the literature. These results indicate that injection of a binary CO_2-N_2 composition
395 is a promising approach to further push CO_2 into the clathrate phase. The kinetics of the
396 proposed process were fully investigated under simulated natural conditions and on real-time
397 scales. This is the first study to analyze the binary gas hydrate formation kinetics in both frozen
398 and unfrozen mesoporous media under realistic conditions. Additionally, the results
399 demonstrate the first experimental evidence backed by thermodynamic modeling results for
400 the formation of sII clathrates by CO_2-N_2 mixed gas with high CO_2 content. Moreover,
401 considering the sudden temperature rise, we found that the presence of N_2 in the system
402 provides a considerably wider safety net for the stability of CO_2 in the clathrate phase.
403 Accordingly, this CCS method reduces the risk of leakage for stored CO_2 into nature, making

it highly attractive for large-scale CCS. Finally, effect of the presence of different salts, and effect of impurities in the injected gas on both hydrate formation and dissociation, and effect of the application of this method on life cycle in the injection environment could be investigated following this work.

Acknowledgements

This work was financially supported by the Skolkovo Institute of Science and Technology, Russia, which is gratefully acknowledged. We thank Dr. Rod Burgass for his valuable contributions to the project. The experiments were conducted at the Centre for Hydrate Research, Institute of Petroleum Engineering, Heriot-Watt University, Edinburgh, United Kingdom.

Author contributions

A.H and J.Y conceived the idea presented in this publication; A.H performed laboratory experiments and analyzed the data; B.T and J.Y supervised the research; A.H and J.Y wrote the manuscript. B.T, E.C, V.I, and B.B discussed the results and contributed to the final manuscript.

References

(1) Myers, S. S.; Zanobetti, A.; Kloog, I.; Huybers, P.; Leakey, A. D. B.; Bloom, A. J.; Carlisle, E.; Dietterich, L. H.; Fitzgerald, G.; Hasegawa, T.; et al. Increasing CO2 Threatens Human Nutrition. *Nature* **2014**, *510* (7503), 139–142, DOI 10.1038/nature13179.

(2) Steinfeld, J. I. *Atmospheric Chemistry and Physics: From Air Pollution to Climate Change*; John Wiley & Sons, 1998; Vol. 40, DOI 10.1080/00139157.1999.10544295.

(3) Hansen, J.; Johnson, D.; Lacis, A.; Lebedeff, S.; Lee, P.; Rind, D.; Russell, G. Climate Impact of Increasing Atmospheric Carbon Dioxide. *Science (80-.).* **1981**, *213* (4511), 957–966, DOI 10.1126/science.213.4511.957.

(4) Notz, D.; Stroeve, J. Observed Arctic Sea-Ice Loss Directly Follows Anthropogenic CO2emission. *Science (80-.).* **2016**, *354* (6313), 747–750, DOI 10.1126/science.aag2345.

(5) Ram, C.; Sivamani, S.; Micha Premkumar, T.; Hariram, V. Computational Study of Leading Edge Jet Impingement Cooling with a Conical Converging Hole for Blade Cooling. *ARPN J. Eng. Appl. Sci.* **2017**, *12* (22), 6397–6406, DOI 10.1039/b000000x.

(6) Myhre, G.; Shindell, D.; Bréon, F. M.; Collins, W.; Fuglestvedt, J.; Huang, J.; Koch, D.; Lamarque, J. F.; Lee, D.; Mendoza, B. *Climate Change 2013: The Physical Science Basis. Contribution of Working Group I to the Fifth Assessment Report of the Intergovernmental Panel on Climate Change*; Cambridge University Press, 2013, DOI 10.1017/CBO9781107415324.

(7) Kvenvolden, K. A.; Lorenson, T. D. The Global Occurrence of Natural Gas Hydrate. In *Geophysical Monograph Series*; 2000; Vol. 124, pp 3–18, DOI 10.1029/GM124p0003.

(8) Zimov, S. A.; Schuur, E. A. G.; Stuart Chapin, F. Permafrost and the Global Carbon Budget. *Science (80-.).* **2006**, *312* (5780), 1612–1613, DOI 10.1126/science.1128908.

(9) Shakhova, N.; Semiletov, I.; Salyuk, A.; Yusupov, V.; Kosmach, D.; Gustafsson, O. Extensive Methane Venting to the Atmosphere from Sediments of the East Siberian Arctic Shelf. *Science (80-.).* **2010**, *327* (5970), 1246–1250, DOI 10.1126/science.1182221.

(10) Maurya, K. K.; Sitholay, O. V. Effect of Schiff Bases on Stabilities of copper(II) Complexes. *Asian J. Chem.* **2007**, *19* (6), 4473–4478, DOI 10.1641/B580807.

(11) Haszeldine, R. S. Carbon Capture and Storage: How Green Can Black Be? *Science (80-.).* **2009**, *325* (5948), 1647–1652, DOI 10.1126/science.1172246.

(12) Boot-Handford, M. E.; Abanades, J. C.; Anthony, E. J.; Blunt, M. J.; Brandani, S.; Mac Dowell, N.; Fernández, J. R.; Ferrari, M. C.; Gross, R.; Hallett, J. P.; et al. Carbon Capture and Storage Update. *Energy Environ. Sci.* **2014**, *7* (1), 130–189, DOI 10.1039/c3ee42350f.

(13) Bui, M.; Adjiman, C. S.; Bardow, A.; Anthony, E. J.; Boston, A.; Brown, S.; Fennell, P. S.; Fuss, S.; Galindo, A.; Hackett, L. A.; et al. Carbon Capture and Storage (CCS): The Way Forward. *Energy Environ. Sci.* **2018**, *11* (5), 1062–1176, DOI 10.1039/C7EE02342A.

(14) Sloan, E. D. Fundamental Principles and Applications of Natural Gas Hydrates. *Nature* **2003**, *426* (6964), 353–359, DOI 10.1038/nature02135.

(15) Mehrabian, H.; Bellucci, M. A.; Walsh, M. R.; Trout, B. L. Effect of Salt on Antiagglomerant Surface Adsorption in Natural Gas Hydrates. *J. Phys. Chem. C* **2018**, *122* (24), 12839–12849, DOI 10.1021/acs.jpcc.8b03154.

(16) Kim, E.; Ko, G.; Seo, Y. Greenhouse Gas (CHF3) Separation by Gas Hydrate Formation. *ACS Sustain. Chem. Eng.* **2017**, *5* (6), 5485–5492, DOI 10.1021/acssuschemeng.7b00821.

(17) House, K. Z.; Schrag, D. P.; Harvey, C. F.; Lackner, K. S. Permanent Carbon Dioxide Storage in Deep-Sea Sediments. *Proc. Natl. Acad. Sci.* **2006**, *103* (33), 12291–12295, DOI 10.1073/pnas.0605318103.

(18) Bai, D.; Zhang, X.; Chen, G.; Wang, W. Replacement Mechanism of Methane Hydrate with Carbon Dioxide from Microsecond Molecular Dynamics Simulations. *Energy Environ. Sci.* **2012**, *5* (5), 7033–7041, DOI 10.1039/c2ee21189k.

(19) Deusner, C.; Bigalke, N.; Kossel, E.; Haeckel, M. Methane Production from Gas Hydrate Deposits through Injection of Supercritical CO2. *Energies* **2012**, *5* (7), 2112–2140, DOI 10.3390/en5072112.

(20) Dornan, P.; Alavi, S.; Woo, T. K. Free Energies of Carbon Dioxide Sequestration and Methane Recovery in Clathrate Hydrates. *J. Chem. Phys.* **2007**, *127* (12), 124510–124700, DOI 10.1063/1.2769634.

(21) Lee, H.; Seo, Y.; Seo, Y. T.; Moudrakovski, I. L.; Ripmeester, J. A. Recovering Methane from Solid Methane Hydrate with Carbon Dioxide. *Angew. Chemie - Int. Ed.* **2003**, *42* (41), 5048–5051, DOI 10.1002/anie.200351489.

(22) Goel, N. In Situ Methane Hydrate Dissociation with Carbon Dioxide Sequestration: Current Knowledge and Issues. *J. Pet. Sci. Eng.* **2006**, *51* (3–4), 169–184, DOI 10.1016/j.petrol.2006.01.005.

(23) Ma, Z. W.; Zhang, P.; Bao, H. S.; Deng, S. Review of Fundamental Properties of CO2 Hydrates and CO2 Capture and Separation Using Hydration Method. *Renew. Sustain. Energy Rev.* **2016**, *53*, 1273–1302, DOI 10.1016/j.rser.2015.09.076.

(24) Schoderbek, D.; Martin, K. L.; Howard, J.; Silpngarmlert, S.; Hester, K. North Slope Hydrate Fieldtrial: CO<inf>2</inf>/CH<inf>4</inf>exchange. In *Society of Petroleum Engineers - Arctic Technology Conference 2012*; Offshore Technology Conference, 2012; Vol. 1.

(25) Yang, J.; Okwananke, A.; Tohidi, B.; Chuvilin, E.; Maerle, K.; Istomin, V.; Bukhanov, B.; Cheremisin, A. Flue Gas Injection into Gas Hydrate Reservoirs for Methane Recovery and Carbon Dioxide Sequestration. *Energy Convers. Manag.* **2017**, *136*, 431–438, DOI 10.1016/j.enconman.2017.01.043.

(26) Hassanpouryouzband, A.; Yang, J.; Tohidi, B.; Chuvilin, E.; Istomin, V.; Bukhanov, B.; Cheremisin, A. CO2 Capture by Injection of Flue Gas or CO2-N2 Mixtures into Hydrate Reservoirs: Dependence of CO2 Capture Efficiency on Gas Hydrate Reservoir Conditions. *Environ. Sci. Technol.* **2018**, *52* (7), 4324–4330, DOI 10.1021/acs.est.7b05784.

(27) Kang, S. P.; Lee, H. Recovery of CO2 from Flue Gas Using Gas Hydrate: Thermodynamic Verification through Phase Equilibrium Measurements. *Environ. Sci. Technol.* **2000**, *34* (20), 4397–4400, DOI 10.1021/es001148l.

(28) Hassanpouryouzband, A.; Yang, J.; Tohidi, B.; Chuvilin, E.; Istomin, V.; Bukhanov, B.; Cheremisin, A. Insights into CO2 Capture by Flue Gas Hydrate Formation: Gas Composition Evolution in Systems Containing Gas Hydrates and Gas Mixtures at Stable Pressures. *ACS Sustain. Chem. Eng.* **2018**, *6* (5), 5732–5736, DOI 10.1021/acssuschemeng.8b00409.

(29) Koh, D. Y.; Kang, H.; Kim, D. O.; Park, J.; Cha, M.; Lee, H. Recovery of Methane from Gas Hydrates Intercalated within Natural Sediments Using CO2 and a CO2/N2 Gas Mixture. *ChemSusChem* **2012**, *5* (8), 1443–1448, DOI 10.1002/cssc.201100644.

(30) Linga, P.; Kumar, R.; Englezos, P. Gas Hydrate Formation from Hydrogen/carbon Dioxide and Nitrogen/carbon Dioxide Gas Mixtures. *Chem. Eng. Sci.* **2007**, *62* (16), 4268–4276, DOI 10.1016/j.ces.2007.04.033.

(31) Babu, P.; Linga, P.; Kumar, R.; Englezos, P. A Review of the Hydrate Based Gas Separation (HBGS) Process Forcarbon Dioxide Pre-Combustion Capture. *Energy* **2015**, *85*, 261–279, DOI 10.1016/j.energy.2015.03.103.

(32) Portnov, A.; Vadakkepuliyambatta, S.; Mienert, J.; Hubbard, A. Ice-Sheet-Driven Methane Storage and Release in the Arctic. *Nat. Commun.* **2016**, *7*, DOI 10.1038/ncomms10314.

(33) Tohidi, B.; Yang, J.; Salehabadi, M.; Anderson, R.; Chapoy, A. CO2hydrates Could Provide Secondary Safety Factor in Subsurface Sequestration of CO2. *Environ. Sci.*

Technol. **2010**, *44* (4), 1509–1514, DOI 10.1021/es902450j.

(34) Dendy Sloan, E.; Koh, C. *Clathrate Hydrates of Natural Gases, Third Edition*; CRC press, 2007; Vol. 20074156, DOI 10.1201/9781420008494.

(35) Schober, H.; Itoh, H.; Klapproth, A.; Chihaia, V.; Kuhs, W. F. Guest-Host Coupling and Anharmonicity in Clathrate Hydrates. *Eur. Phys. J. E* **2003**, *12* (1), 41–49, DOI 10.1140/epje/i2003-10026-6.

(36) Chazallon, B.; Pirim, C. Selectivity and CO2 Capture Efficiency in CO2-N2 Clathrate Hydrates Investigated by in-Situ Raman Spectroscopy. *Chem. Eng. J.* **2018**, *342*, 171–183, DOI 10.1016/j.cej.2018.01.116.

(37) Seo, Y.-T.; Lee, H. Structure and Guest Distribution of the Mixed Carbon Dioxide and Nitrogen Hydrates As Revealed by X-Ray Diffraction and ^{13}C NMR Spectroscopy. *J. Phys. Chem. B* **2004**, *108* (2), 530–534, DOI 10.1021/jp0351371.

(38) Seo, Y. T.; Moudrakovski, I. L.; Ripmeester, J. A.; Lee, J. W.; Lee, H. Efficient Recovery of CO2 from Flue Gas by Clathrate Hydrate Formation in Porous Silica Gels. *Environ. Sci. Technol.* **2005**, *39* (7), 2315–2319, DOI 10.1021/es049269z.

(39) Lee, Y.; Lee, S.; Lee, J.; Seo, Y. Structure Identification and Dissociation Enthalpy Measurements of the CO2+N2 Hydrates for Their Application to CO2 Capture and Storage. *Chem. Eng. J.* **2014**, *246*, 20–26, DOI 10.1016/j.cej.2014.02.045.

(40) Waite, W. F.; Santamarina, J. C.; Cortes, D. D.; Dugan, B.; Espinoza, D. N.; Germaine, J.; Jang, J.; Jung, J. W.; Kneafsey, T. J.; Shin, H.; et al. Physical Properties of Hydrate-Bearing Sediments. *Rev. Geophys.* **2009**, *47* (2008), RG4003, DOI 10.1029/2008RG000279.Table.

(41) Kasting, J. F.; Howard, M. T.; Wallmann, K.; Veizer, J.; Shields, G.; Jaffrés, J. Paleoclimates, Ocean Depth, and the Oxygen Isotopic Composition of Seawater. *Earth Planet. Sci. Lett.* **2006**, *252* (1–2), 82–93, DOI 10.1016/j.epsl.2006.09.029.

(42) Resing, J. A.; Sedwick, P. N.; German, C. R.; Jenkins, W. J.; Moffett, J. W.; Sohst, B. M.; Tagliabue, A. Basin-Scale Transport of Hydrothermal Dissolved Metals across the South Pacific Ocean. *Nature* **2015**, *523* (7559), 200–203, DOI 10.1038/nature14577.

(43) Haghighi, H.; Chapoy, A.; Burgess, R.; Tohidi, B. Experimental and Thermodynamic Modelling of Systems Containing Water and Ethylene Glycol: Application to Flow Assurance and Gas Processing. *Fluid Phase Equilib.* **2009**, *276* (1), 24–30, DOI 10.1016/j.fluid.2008.10.006.

(44) Mahabadian, M. A.; Chapoy, A.; Burgass, R.; Tohidi, B. Development of a Multiphase Flash in Presence of Hydrates: Experimental Measurements and Validation with the CPA Equation of State. *Fluid Phase Equilib.* **2016**, *414* (JANUARY), 117–132, DOI 10.1016/j.fluid.2016.01.009.

(45) Hassanpouryouzband, A.; Farahani, M. V.; Yang, J.; Tohidi, B.; Chuvilin, E.; Istomin, V.; Bukhanov, B. Solubility of Flue Gas or Carbon Dioxide-Nitrogen Gas Mixtures in Water and Aqueous Solutions of Salts: Experimental Measurement and Thermodynamic Modeling. *Ind. Eng. Chem. Res.* **2019**, acs.iecr.8b04352, DOI 10.1021/acs.iecr.8b04352.

(46) Tung, Y.-T.; Chen, L.-J.; Chen, Y.-P.; Lin, S.-T. The Growth of Structure {I} Methane Hydrate from Molecular Dynamics Simulations. *J. Phys. Chem. B* **2010**, *114* (15), 10804–10813, DOI 10.1021/jp112205x.

(47) Kennett, J. P. *Abstract: Methane Hydrates in Quaternary Climate Change: The Clathrate Gun Hypothesis*; Wiley Online Library, 2005.

Synopsis

More than 92 mol% of the CO_2 present in power plant flue gas could be stored without pre capture by formation of flue gas hydrates in permafrost regions.

For Table of Contents Use Only